

- 306 (1972).
- ³L. F. Mattheiss, Phys. Rev. **181**, 987 (1969).
- ⁴J. C. Slater and G. F. Koster, Phys. Rev. **94**, 1498 (1954).
- ⁵L. F. Mattheiss, Phys. Rev. B **2**, 3918 (1970).
- ⁶F. Herman and S. Skillman, *Atomic Structure Calculations* (Prentice-Hall, Englewood Cliffs, N. J., 1963).
- ⁷P. D. DeCicco, Phys. Rev. **153**, 931 (1967).
- ⁸J. C. Slater, *Quantum Theory of Molecules and Solids*, Vol. 2 (McGraw-Hill, New York, 1965).
- ⁹J. C. Slater, Phys. Rev. **81**, 385 (1951).
- ¹⁰H. O. Hartley, Technometrics **3**, 269 (1961).
- ¹¹V. Heine and L. F. Mattheiss, J. Phys. C **4**, L191 (1971).
- ¹²E. I. Zornberg, Phys. Rev. B **1**, 244 (1970).
- ¹³J. M. Tyler, T. E. Norwood, and J. L. Fry, Phys. Rev. B **1**, 297 (1970).
- ¹⁴T. E. Norwood and J. L. Fry, Phys. Rev. B **2**, 472 (1970).
- ¹⁵S. Sugano and R. G. Shulman, Phys. Rev. **130**, 517 (1963).
- ¹⁶J. L. Fry (private communication).
- ¹⁷V. Ern and A. C. Switendick, Phys. Rev. **137**, A1927 (1965).
- ¹⁸J. M. Schoen and S. P. Denker, Phys. Rev. **184**, 864 (1969).
- ¹⁹T. M. Wilson, Intern. J. Quantum Chem. **3**, 757 (1970); J. Appl. Phys. **40**, 1588 (1969).
- ²⁰A. C. Switendick, Quarterly Progress Report, Solid-State and Molecular Theory Group, MIT, Vol. 49, p. 41, 1963 (unpublished).
- ²¹J. Yamashita, J. Phys. Soc. Japan **18**, 1010 (1963).
- ²²D. Adler and J. Feinleib, Phys. Rev. B **2**, 3112 (1970).

PHYSICAL REVIEW B

VOLUME 5, NUMBER 2

15 JANUARY 1972

Electronic Structure of the 3d Transition-Metal Monoxides.

II. Interpretation

L. F. Mattheiss

Bell Laboratories, Murray Hill, New Jersey 07974

(Received 5 August 1971)

The results of augmented-plane-wave (APW) energy-band calculations for the 3d transition-series monoxides CaO, TiO, VO, MnO, FeO, CoO, and NiO are interpreted in terms of the electrical and optical data for these compounds. A detailed analysis of the effects of a crystalline field on the nonmagnetic *d* bands in the rocksalt structure shows that these bands are not split into nonoverlapping e_g and t_{2g} bands by a cubic field. Instead, these effects broaden the *d* bands in such a way that each of these compounds with partially filled *d* bands should exhibit metallic behavior. This model is consistent with the insulating properties of CaO and the metallic behavior of TiO and VO. However, the observed electrical and optical properties of MnO, FeO, CoO, and NiO suggest that these materials are Mott insulators, despite the fact that the present calculations predict 3d bandwidths $W \approx 3$ eV. Assuming that the 3d electrons in these materials are in localized Wannier rather than itinerant Bloch states, the APW energy bands are used to calculate the crystal-field parameters Δ for these insulating compounds, where Δ is the difference in the average energies of the e_g and t_{2g} bands. This leads to calculated values for Δ which are consistently 30% smaller than the experimental values. One interpretation of this discrepancy suggests that the true 3d bandwidths W are closer to 4 eV rather than 3 eV for these insulating compounds. Hubbard's simplified model calculations show that a Mott transition occurs when $W \approx U$, the Coulomb interaction energy between two electrons on the same atom. The fact that MnO to NiO are Mott insulators implies that $U > 4$ eV in these compounds.

I. INTRODUCTION

In the preceding paper¹ (hereafter referred to as I), the results of augmented-plane-wave (APW) energy-band calculations for the 3d transition-series monoxides CaO to NiO are presented. The purpose of the present paper is to interpret these energy-band results in terms of the electrical and optical data that is currently available for these compounds.

It has been found experimentally that these 3d transition-metal monoxides include materials with rather diverse and interesting physical properties. The series begins with CaO, which is a typical

Bloch-Wilson insulator. Based on their reflectance measurements, Whited and Walker² estimate a band gap of 7 eV separating the oxygen 2*p* valence bands and the unoccupied calcium 3*d* and 4*s*-4*p* conduction bands. Strong exciton peaks obscure the actual band edge, and Van Vechten³ has assigned a direct gap of 9.8 eV for this compound. However, the observation by Janin and Cotton⁴ of a threshold for photoconductivity at 6.2 eV in powdered samples suggests a lower value for the band gap.

The next two members of this series, TiO and VO, exhibit metallic-type conductivity down to liquid-helium temperatures. There were early reports of a metal-insulator transition in VO near

120 °K,^{5,6} but recent studies⁷ indicate that no such transition occurs in VO samples that are known to have the rocksalt structure. It is believed that the samples involved in the early measurements contained V₂O₃.⁷ Both TiO and VO form with the rocksalt structure over wide ranges of stoichiometry. Even when they are formed stoichiometrically, they still contain about 15% vacancies on both the metal and oxygen sublattices.⁷ These imperfections prevent the application of the de Haas–van Alphen effect and similar techniques to study the Fermi surfaces of these metallic compounds. Doyle *et al.*⁸ have found that they can remove all the vacancies in stoichiometric TiO by annealing at high temperatures and pressures, which indicates that it may be possible to prepare good single crystals for future Fermi-surface studies.

The last four members of this series, MnO, FeO, CoO, and NiO, are antiferromagnetic insulators. They fail to exhibit metallic-type conductivity, even at temperatures above their Néel temperatures. The optical absorption spectra below 4 eV have been studied for MnO,^{9,10,11} FeO,⁹ and NiO^{12–14} and interpreted in terms of crystal-field transitions between the ground- and excited-state multiplets of the corresponding free ion by including a crystal-field splitting Δ between the e_g and t_{2g} orbital energies. It is found that the positions of the peaks in the absorption spectra are shifted only slightly when traces of Ni^{14,15} and Co¹⁶ are introduced substitutionally into MgO crystals.

These properties are very difficult to explain in terms of a band model for the 3d electrons in these compounds. All calculations of the nonmagnetic energy bands for the 3d transition-metal monoxides^{1,17–21} yield overlapping, partially filled 3d bands. For the compounds MnO, FeO, CoO, and NiO, this implies metallic behavior above the Néel temperature, where the effects of the magnetic superlattice should disappear. This situation was anticipated by Mott,²² who proposed that electron-electron correlation effects cause the 3d electrons to form a ground state made up of localized atomic-like rather than itinerant Bloch functions. Morin²³ proposed a similar idea, based on the observation that there is a trend in the 3d transition-metal monoxide series from metals to insulators as the nuclear charge is increased. He attributed this trend to a contraction in the 3d orbital radii with increasing nuclear charge which, according to Mott's proposal, will finally lead to an abrupt change from metallic to insulating behavior.

Much of the earlier literature dealing with experimental results for transition-metal oxides and the theoretical models that have been proposed to explain them are summarized in the review article by Adler.²⁴ In a more recent article, Adler and Feinleib²⁵ apply a localized 3d model to interpret the

electrical and optical properties of MnO, FeO, CoO, and NiO. They propose a model in which the 3d bandwidth is extremely narrow in these materials, and they treat correlation effects between the 3d electrons using an approach suggested by Hubbard.²⁶ On the other hand, Slater²⁷ has suggested that the electronic properties of these materials can be understood in terms of spin-polarized energy bands. Wilson²⁸ has shown that this approach predicts that MnO and NiO are semiconductors below their Néel temperatures and argues that this result will persist above their Néel temperatures as well.

In the first part of the present paper, we consider the effects of the crystalline field on the d bands in the rocksalt structure. These effects are important because the e_g and t_{2g} bands cannot overlap if NiO is to remain insulating in the paramagnetic state above the Néel temperature according to Wilson's spin-polarized band model for NiO. It is shown that a cubic field will not split the d bands into nonoverlapping e_g and t_{2g} bands in the rocksalt structure, regardless of the strength of this field. In the second part of this paper, we review some of the experimental data on these compounds and comment on various aspects of the theoretical models that have been introduced to explain them. It is argued that the spin-polarized band model will predict FeO and CoO to have partially filled t_{2g} bands, even in the antiferromagnetic state. It is suggested that the 3d electrons in MnO, FeO, CoO, and NiO must be described in terms of localized Wannier rather than itinerant Bloch states. The APW energy-band results are used to determine the energies of the e_g and t_{2g} Wannier functions, which correspond to the average energies of the e_g and t_{2g} bands, respectively. The difference between the energies of the e_g and t_{2g} Wannier functions is identified with the crystal-field parameter Δ , which can be compared with the experimental values determined from the absorption spectra. It is found that the calculated values for Δ are consistently 30% smaller than the experimental results. Since Δ is approximately proportional to the 3d bandwidth, this implies that the actual 3d bandwidths W for these insulating oxides are about 4 eV. In terms of Hubbard's estimate that $W \approx U$ at the Mott transition for a half-filled s band,²⁶ these results set a lower limit for U (the Coulomb repulsion energy between two electrons on the same atom) in these compounds at about 4 eV.

There are two features in the energy band results for the 3d transition-series monoxides that suggest a localized model for the 3d electrons in MnO, FeO, CoO, and NiO. First, it is found that the 3d bandwidths for the metallic oxides TiO and VO are about two and a half times larger than those for the insulating oxides MnO to NiO. Second, it is found that the bottom of the metal 4s-4p band overlaps the 3d bands in the metallic but not the insulating oxides.

It has been suggested²⁹ that this overlap plays an important role in destroying the Mott insulator state.

II. CRYSTAL-FIELD EFFECTS: ROCKSALT AND PEROVSKITE STRUCTURES

It is a well-known result of crystal-field theory that the five d levels of a transition-metal atom or ion are split into a triply degenerate t_{2g} and a doubly degenerate e_g level by a cubic field. This result has been extended to energy-band theory by means of semi-intuitive arguments. Namely, it has been assumed that the d bands in a transition-metal compound can always be split into nonoverlapping e_g and t_{2g} subbands provided that the d bands are sufficiently narrow and the crystal field is sufficiently strong. There is a tendency to associate crystal-field splittings in cubic systems with the energy separation between the energy-band states at the center of the Brillouin zone, namely those with Γ_{12} and $\Gamma_{25'}$ symmetry, respectively. Finally, there is considerable discussion and controversy concerning the origin of these crystal-field splittings, both in crystals as well as in isolated molecular complexes.

In the present analysis, we show that an octahedral field can split the e_g and t_{2g} bands in the ReO_3 and perovskite structures but not in the rocksalt structure. In addition, it is shown that crystal-field effects cause a broadening of the d bands which is similar to that which results from direct d - d interactions. This is clear from the discussion of effective d - d interactions in I. Finally, it is argued that the crystal-field splitting is associated not with the energy separation at Γ but rather with the difference between the average e_g and t_{2g} band energies. It has been shown³⁰ that this corresponds to the crystal-field parameter Δ that is obtained from molecular-orbital (MO) calculations on isolated octahedral transition-metal complexes.

To illustrate the effects of the lattice periodicity on the crystal-field levels of an isolated complex, we apply the linear-combination-of-atomic-orbitals (LCAO) method of I and compare these results with those obtained from the MO method. According to both approaches, the crystal-field effects are due to overlap and covalency between the transition-metal d and ligand s and p orbitals and can be described in terms of three parameters Δ_s , Δ_p , and Δ_π .³⁰ We consider both the ReO_3 -perovskite and rocksalt structures. Both contain a metal atom that is surrounded by a perfect octahedron of neighboring ligands. The two structures differ only in the way in which these octahedra are stacked together to form a three-dimensional periodic lattice. In the ReO_3 and perovskite structures, the neighboring octahedra share vertices along $\langle 100 \rangle$, which leads to a simple cubic bravais lattice with one ReO_3 complex per unit cell. The perovskite structure con-

tains an alkali or alkaline earth atom at the corners of this cell. In the rocksalt or sodium-chloride structure, the neighboring octahedra share edges along $\langle 110 \rangle$ and vertices along $\langle 100 \rangle$, and this leads to an fcc bravais lattice with a single NaCl molecule per unit cell.

In these octahedrally coordinated compounds, the strongest interactions are those between electrons on the metal atom and those on its six neighboring ligands. This is clear from the results of Table IV in I. In the MO and LCAO methods, these interactions are represented by the two-center energy integrals ($s\sigma$), ($p\delta\sigma$), and ($pd\pi$) and the corresponding orbital overlap integrals S_s , S_p , and S_π , respectively. It has been shown³⁰ that the energy integrals ($s\sigma$), ($p\delta\sigma$), and ($pd\pi$) involving nonorthogonal orbitals can be related to their orthogonalized equivalents ($s\sigma$ '), ($p\delta\sigma$ '), and ($pd\pi$)' by the expressions

$$(s\sigma) = \frac{1}{2}S_s(E_s + E_d) + (s\sigma)', \quad (1a)$$

$$(p\delta\sigma) = \frac{1}{2}S_p(E_p + E_d) + (p\delta\sigma)', \quad (1b)$$

$$(pd\pi) = \frac{1}{2}S_\pi(E_p + E_d) + (pd\pi)', \quad (1c)$$

where E_s , E_p , and E_d are the ligand s and p and metal d orbital energies, respectively. It is clear that ($s\sigma$) = ($s\sigma$)' if $S_s = 0$, etc. According to Eq. (1), the parameters ($s\sigma$), ($p\delta\sigma$), and ($pd\pi$) depend on the zero of energy. However, this energy dependence is such that it exactly cancels a similar term that is introduced into the Hamiltonian matrix by the transformation from a nonorthogonal to an orthonormal basis and this leads to a band structure that shifts rigidly with the zero of energy.

In Fig. 1, we compare the crystal-field levels of an isolated complex with the gross features of the energy bands for the rocksalt and perovskite (ReO_3) structures. First, we consider the results for the isolated complex in the center portion of the figure. Neglecting metal-ligand interactions, we have the atomiclike energy levels E_d , E_p , and E_s that are shown to the left of the dashed lines. The crystal-line environment splits E_d into e_g and t_{2g} levels and E_p into σ and π levels. The energies of the e_g and t_{2g} levels correspond to $E_{3z^2-r^2}$ and E_{xy} in Table II of I. The fact that $E_{3z^2-r^2} < E_{xy}$ was first pointed out by Kleiner.³¹ The metal-ligand interactions shift the t_{2g} level by an amount $\frac{1}{2}\Delta_\pi$, where to second order

$$\Delta_\pi = 8 \left[\frac{1}{2}S_\pi(E_d - E_p) - (pd\pi)' \right]^2 / (E_d - E_p). \quad (2)$$

It has been shown previously³⁰ that ($pd\pi$)' and S_π have opposite signs so that the two terms in square brackets add when $(E_d - E_p)$ is positive. The corresponding shift of the $p\pi$ valence level is given by an expression similar to Eq. (2) except that it contains a + rather than a - sign. As a result, the shift of the $p\pi$ valence level is reduced by cancellation between the overlap and covalency contributions.

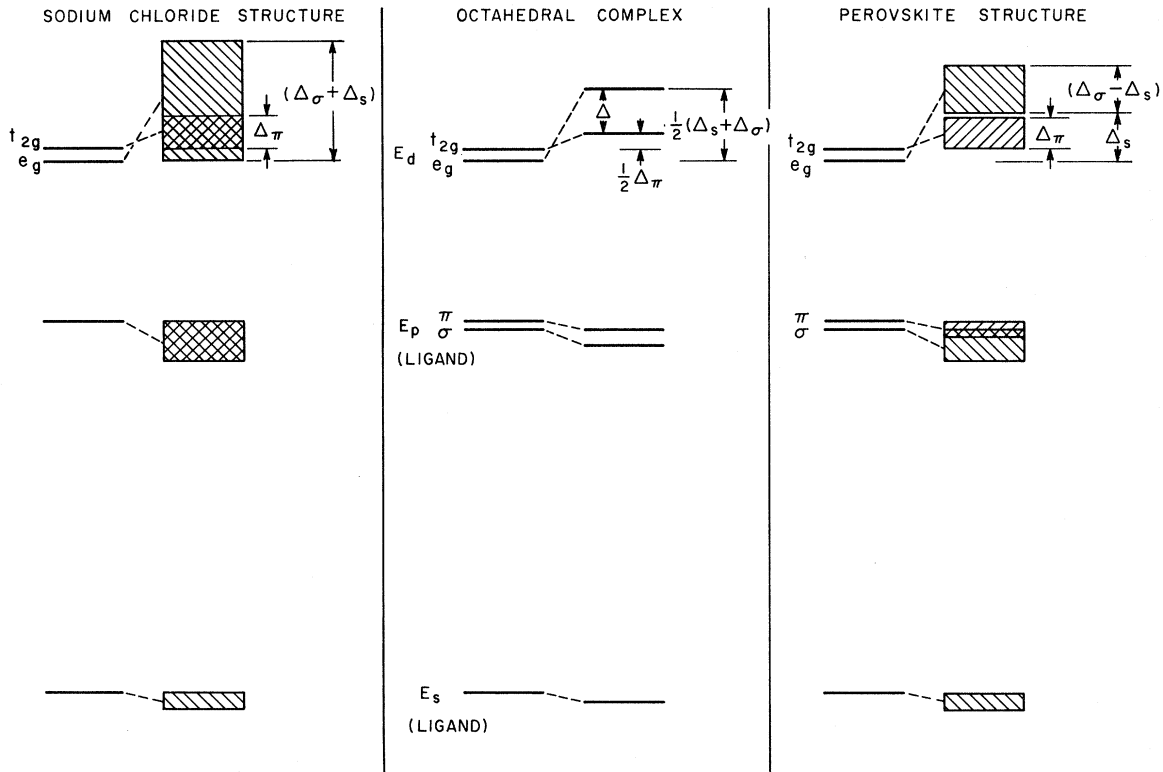


FIG. 1. Comparison between crystal-field effects in an isolated octahedral complex and the energy bands for the rocksalt and ReO_3 -perovskite structures.

The stronger σ interactions shift the energy of the e_g level by a much larger amount $\frac{1}{2}(\Delta_s + \Delta_\sigma)$, where to second order

$$\Delta_s = 6 \left[\frac{1}{2} S_s (E_d - E_s) - (sd\sigma)' \right]^2 / (E_d - E_s), \quad (3)$$

$$\Delta_\sigma = 6 \left[\frac{1}{2} S_\sigma (E_d - E_p) - (pd\sigma)' \right]^2 / (E_d - E_p). \quad (4)$$

Again, the shift of the $p\sigma$ and $s\sigma$ valence levels is reduced by similar cancellation effects. The final crystal-field splitting Δ between the e_g and t_{2g} levels is given by the expression

$$\Delta = E_{3z^2-r^2} - E_{xy} + \frac{1}{2}(\Delta_s + \Delta_\sigma - \Delta_\pi). \quad (5)$$

According to the results of Table V in I, Δ is also equal to $\mathcal{E}_{3z^2-r^2, 3z^2-r^2}(000) - \mathcal{E}_{xy, xy}(000)$.

The effect of the lattice periodicity on these crystal-field levels is shown to the right for the ReO_3 and perovskite structures. For simplicity, direct metal-metal and ligand-ligand contributions to the band structure are neglected. It is found that the wave-vector dependence of the metal-ligand π interactions broadens the t_{2g} level into a band of width Δ_π . The width of the $p\pi$ valence band (indicated by the similar cross-hatching) is reduced by the same cancellation effects that were described earlier. The metal-ligand σ interactions shift the e_g level by an amount Δ_s and broaden it into a band

of width $(\Delta_\sigma - \Delta_s)$. The splitting between the e_g and t_{2g} bands is complete if $\Delta_s > \Delta_\sigma$. The dotted lines connect the e_g and t_{2g} levels with the average energies of the e_g and t_{2g} bands. The differences between these average e_g and t_{2g} band energies is exactly the crystal-field splitting Δ for the isolated octahedral complex if direct $d-d$ interactions are neglected. In the ReO_3 and perovskite structures, the average e_g and t_{2g} band energies can be determined directly from the energy-band results at the center (Γ) and corner (R) of the simple cubic Brillouin zone. It is easily shown that the average e_g and t_{2g} band energies are $\frac{1}{2}[E(\Gamma_{12}) + E(R_{12})]$ and $\frac{1}{2}[E(\Gamma_{25'}) + E(R_{25'})]$, respectively, so that

$$\Delta = \frac{1}{2}[E(\Gamma_{12}) + E(R_{12}) - E(\Gamma_{25'}) - E(R_{25'})] \quad (6)$$

for the ReO_3 and perovskite structures.

To the left in Fig. 1, the analogous results for the rocksalt structure are illustrated. As in the ReO_3 structure, the t_{2g} level is broadened to form a band of width Δ_π . However in this case, the e_g bandwidth is proportional to $(\Delta_s + \Delta_\sigma)$ and the e_g and t_{2g} bands overlap. This is due to the fact that the metal-ligand overlap and covalency interactions vanish at the center of the Brillouin zone Γ . It is shown in I that the small energy difference between the e_g and t_{2g} states at Γ (Γ_{12} and $\Gamma_{25'}$, re-

spectively) is due entirely to nearest-neighbor d - d interactions and the parameter $\gamma = E_{3z^2-r^2} - E_{xy}$. The strong metal-ligand interactions raise the e_g and t_{2g} bands at other points in the zone; this effect causes the e_g and t_{2g} bands to overlap, regardless of the strength of the crystal field. Once again the difference between the average e_g and t_{2g} band energies is equal to Δ . However, in this case, the average e_g and t_{2g} band energies are not related in any simple way to the energy-band results at symmetry points in the Brillouin zone. Consequently, one cannot determine these average energies as easily as they are determined in the ReO_3 and perovskite structures. However, the LCAO interpolation method provides a convenient procedure for determining these average energies. According to the analysis in I, the average e_g and t_{2g} energies are given by the effective LCAO parameters $\mathcal{E}_{3z^2-r^2, 3z^2-r^2}(000)$ and $\mathcal{E}_{xy, xy}(000)$ of Table V, respectively. Finally, in the rocksalt structure there is no distinction between the $p\sigma$ and $p\pi$ valence bands since those orbitals which form a σ bond with one metal atom form π bonds with its neighbors.

From this comparison, it is clear that the effects of the crystal field on the energy bands are strongly dependent on the crystal structure. One interesting feature of the LCAO method with non-orthogonal orbitals is that it can be applied not only as an interpolation method, but also as an extrapolation method. Thus, the LCAO parameters of Table IV in I which have been determined by fitting the APW results for the MO-type monoxides can be applied to predict the band structures for a MO_3 -type stacking of octahedra. A simple analysis of the results in Tables IV-VI in I predicts that the e_g and t_{2g} bands for these MO_3 compounds will be split since $(E_{3z^2-r^2} + \Delta_s) > (E_{xy} + \Delta_\pi)$ for all six compounds. In applying the LCAO method as an extrapolation procedure, one must take into account the fact that the direct d - d interactions are larger in the rocksalt structure because the metal-metal distance is reduced by the factor $\frac{1}{2}\sqrt{2}$ from that in the ReO_3 structure and there is no ligand atom located between the nearest-neighbor metal atoms.

III. EXPERIMENTAL DATA AND THEIR INTERPRETATION

A. CaO

The most detailed experimental results for CaO are the reflectance data of Whited and Walker,² which span an energy range extending from 6 to 35 eV. They observe peaks in the reflectance at energies of 6.8, 10, 11.4, 13, 17, 27, and 35 eV. These data have been analyzed to obtain the real and imaginary parts of the dielectric function, ϵ_1 and ϵ_2 , respectively. The two peaks in the ϵ_2 spectrum at 6.8 and 11.4 eV are attributed to ex-

citons; the remaining structure is assigned to interband transitions. Whited and Walker tentatively assign the 6.8- and 11.4-eV excitons to the $X_5' - X_3$ and $X_4' - X_3$ band gaps, respectively. (See Fig. 6 of I). If the binding energies for these excitons are assumed to be equal, this implies that $E(X_5') - E(X_4') = 4.6$ eV. The present APW results for CaO yield a much smaller value for this energy difference, namely 0.3 eV. Thus, these APW energy bands for CaO are in serious disagreement with this interpretation of the exciton spectra.

By assuming an 0.5-eV binding energy for these excitons, Whited and Walker estimate that the direct band gaps at Γ and X are 7.0 and 7.3 eV, respectively. These values are nearly 3 eV smaller than the calculated direct gaps of 9.7 eV, which are nearly the same at both Γ and X . Thus, the present calculations confirm one aspect of their band model, the fact that the bottom of the $4s$ and $3d$ bands are nearly degenerate. Although Van Vechten³ assigns a direct gap of 9.8 eV for CaO, the fact that Janin and Cotton⁴ observe a photoconductivity threshold at 6.2 eV indicates that the actual gap is several electron volts smaller.

In assigning the remaining structure in the ϵ_2 spectrum to interband transitions, Whited and Walker rely on the empirical pseudopotential band structure for MgO, as determined by Fong *et al.*³² from the ϵ_2 spectrum of that material. Whited and Walker propose a band structure for CaO in which the oxygen $2p$ bandwidth is about 7 eV and the calcium $3d$ bandwidth is in the 10-15-eV range. The present APW results yield $2p$ and $3d$ bandwidths of 1.1 and 5.8 eV, respectively, for CaO. Thus, the APW band structure predicts that p to d transitions will extend over a much smaller energy range (about 7 eV) beyond the band gap, namely from 9.7 to 16.6 eV. This includes the energy range where structure is observed in the experimental ϵ_2 spectrum. At higher energies, the present APW calculations predict transitions between the calcium $3s$, $3p$, and oxygen $2s$ core levels and the conduction bands starting at 41, 23, and 25 eV, respectively. This indicates a possible interpretation of the higher energy peaks in the reflectance that are observed at 27 and 35 eV.

B. TiO and VO

The compounds TiO_x and VO_x exist with the rocksalt structure over wide ranges of stoichiometry. It is found that x can be varied between 0.8 and 1.3 and this leads to significant changes in the physical properties of these materials. This has led to serious discrepancies between independent measurements of the various properties of these materials, as emphasized by Banus and Reed.⁷ In addition to deviations from stoichiometry, TiO and VO also contain substantial numbers of vacancies

on both the metal and oxygen sublattices. In the case of stoichiometric TiO samples, it is possible to reduce the vacancy concentration by annealing at high temperatures and pressures.^{7,8} Apparently, this is not possible in VO.⁷ In both materials, it is found that the lattice parameter increases as the vacancy concentration is reduced.

Banus and Reed have studied the temperature and composition dependence of the resistivity and magnetic susceptibility of TiO and VO. While these properties are quite independent of temperature and composition for TiO_x they find that VO_x exhibits a gradual change from metallic to semiconducting behavior as *x* is increased from 1 to 1.3. It is not clear if this is an intrinsic property of the material or one that is due to the increasing vacancy concentration at the vanadium sites that occurs in this range of *x* values.

Fischer³³ has interpreted the x-ray *K* and *L* emission bands and absorption spectra for TiO. He attributes peaks in the emission spectra at energies 8 and 23 eV below the TiO Fermi energy to the oxygen 2*p* and 2*s* bands, respectively. These coincide very closely with the positions of these bands in the energy-band results of Ern and Switendick¹⁹ for TiO. The present calculations for TiO place these peaks at 11.5 and 26 eV below the Fermi energy. If Fischer's interpretation is correct, this suggests that the present calculations overestimate the 2*p*-3*d* band gap by 3 eV in TiO.

C. MnO, FeO, CoO, and NiO

The main difficulty in applying a band model to MnO, FeO, CoO, and NiO is that of explaining their insulating properties in the antiferromagnetic and paramagnetic states. This is especially true above the Néel temperature where the lattice distortions and the antiferromagnetic superlattice effects disappear. Slater²⁷ has argued that such an explanation is possible in terms of a spin-polarized energy-band model. Slater has shown that the exchange splitting between the energy bands for the 3*d* electrons with spin up (parallel to the local magnetization) and spin down (antiparallel) is determined by the intra-atomic exchange integrals which are responsible for the multiplet structure in the isolated atoms or ions. Since this is intrinsically an atomic property, Slater argues that this splitting will persist in the paramagnetic state above the Néel temperature and could explain the insulating properties of MnO and NiO if the cubic field were sufficiently strong to split the 3*d* band into nonoverlapping *e_g* and *t_{2g}* bands. According to Slater, the splitting Δ_{ex} between the spin-up and spin-down bands is given by

$$\Delta_{\text{ex}} = (q_{\uparrow} - q_{\downarrow}) \frac{1}{14} [F^2(3d; 3d)_{\uparrow} + F^4(3d; 3d)], \quad (7)$$

where *q_↑* and *q_↓* are the numbers of spin-up and

spin-down electrons, respectively, and *F*² and *F*⁴ are the usual Slater integrals involved in atomic multiplet theory. Herring³⁴ has criticized this method for estimating Δ_{ex} because it omits an important contribution from the *F*⁰(3*d*; 3*d*) integral (or *U*, as it is referred to here). Herring claims that Eq. (7) is appropriate for an atom or ion but not a solid. This question is still unresolved.

Wilson²⁸ has applied the spin-polarized energy-band model to calculate the antiferromagnetic band structures of MnO and NiO using the APW method. He finds that the 3*d* bands, which have a width of about 0.15 Ry, are split by the intra-atomic exchange effects into spin-up and spin-down subbands that are separated by 0.4 Ry in MnO and 0.3 Ry in NiO. Wilson also finds that the *e_g* and *t_{2g}* bands do not overlap so that both MnO and NiO have completely filled bands separated by an energy gap in the one-electron density of states. In the case of MnO, the spin-up *e_g* and *t_{2g}* bands are filled and separated by a 0.3-Ry gap from the bottom of the manganese 4*s* band and 0.4 Ry from the spin-down *e_g* and *t_{2g}* bands. In NiO, the spin-up *e_g* and *t_{2g}* and spin-down *t_{2g}* bands are filled, and the band gap is that which is between the spin-down *t_{2g}* and *e_g* bands.

Despite its successful application to MnO and NiO, this spin-polarized band model possesses several difficulties. First, if Wilson's model is generalized and applied to the intermediate compounds FeO and CoO, it predicts that these compounds will have partially filled spin-down *t_{2g}* bands, even in the antiferromagnetic state. Second, it has been shown that the crystal field should not split the *d* band in the rocksalt structure. Therefore, it is concluded that the splitting between the *e_g* and *t_{2g}* bands which occurs in Wilson's calculation is due to the magnetic superlattice and this splitting should disappear above the Néel temperature, thereby causing NiO to be metallic in this temperature range. Wilson estimates the crystal-field parameter Δ from the difference in the *e_g* and *t_{2g}* band energies at the center of the zone. In the case of MnO, it is difficult to see how this energy difference could be involved in the optical absorption spectra since these bands are either completely filled (spin up) or completely empty (spin down). Finally, it is not clear how a band model can explain the crystal-field multiplet structure that is observed in the low-energy absorption spectra for these materials. A band model has even more difficulty explaining the fact that these absorption peaks shift only slightly when dilute traces of Co and Ni are substituted into an MgO host.¹⁴⁻¹⁶

These difficulties with the spin-polarized band model suggest that the 3*d* electrons in MnO, FeO, CoO, and NiO are localized rather than itinerant.

TABLE I. Contributions to the calculated values of the crystal-field parameters Δ and their comparison with experiment (in rydbergs).

| | MnO | FeO | CoO | NiO |
|------------------------------------|-----------------------|--------|--------------------|--------------------|
| $E_{3d^2-r^2} - E_{xy}$ | -0.015 | -0.014 | -0.012 | -0.011 |
| $\frac{1}{2}(\Delta_g + \Delta_o)$ | 0.087 | 0.090 | 0.084 | 0.083 |
| $-\frac{1}{2}\Delta_r$ | -0.015 | -0.017 | -0.016 | -0.016 |
| Δ_{calc} | 0.057 | 0.059 | 0.056 | 0.056 |
| | 0.089 ^{a, b} | | 0.086 ^a | 0.083 ^c |
| Δ_{expt} | 0.092 ^d | | | 0.081 ^e |
| | | | | 0.080 ^f |

^aReference 9.

^bReference 11.

^cReference 12.

^dReference 10.

^eReference 13.

^fReference 14.

The LCAO method can be applied to determine the energies of the e_g and t_{2g} Wannier functions, as described in Sec. II. The difference between the energies of the e_g and t_{2g} Wannier functions is the crystal-field parameter Δ , which can be compared with the experimental values that are determined from the absorption spectra. These results for MnO, FeO, CoO, and NiO are summarized in Table I. It is found that the calculated values for Δ are nearly constant for the series MnO to NiO and are about 30% smaller than the experimental values. The experimental values exhibit about a 10% decrease from MnO to NiO.

There are several possible explanations for the discrepancies between these calculated and experimental values for Δ . The simplest explanation is to assume that the present calculations overestimate the $2p$ - $3d$ band gap. A reduction in this gap would increase the crystal-field parameters Δ_s , Δ_o , and Δ_r of Eqs. (2)-(4) by reducing the magnitude of the energy denominators. It is clear that such a change would also increase the $3d$ bandwidth. However, this discrepancy could also be due to a simplifying assumption that is made in crystal-field theory. Namely, it is normally assumed that the e_g and t_{2g} orbitals have the same radial wave function. This approximation reduces the number of parameters that are required to fit the optical spectra to a minimum number of three.³⁵ These parameters include Δ as well as the Racah parameters B and C , where B and C are simply related to the Slater F^2 and F^4 integrals.³⁵ It is only in this approximation that, for example, the lowest energy ${}^3A_2 \rightarrow {}^3T_2$ transition in NiO is equal to the crystal-field parameter Δ . Since the absorption spectra for these materials usually contain only six or seven peaks, this approximation is essential if the fitting procedure is to involve fewer parameters than the total number of observed peaks.

Stephens and Drickamer¹³ have measured the effect of pressure on Δ for NiO. They find that Δ is

increased by 10% at a pressure of 130 kbar, which corresponds to a 2% decrease in the lattice constant.³⁶ To estimate the way in which Δ will vary with the lattice parameter, I have used the results of two APW calculations for VO, one for the observed lattice parameter and the other for a value that is 12% larger.²⁹ A linear extrapolation of the Δ 's obtained from these calculations predicts that Δ will increase by 8% if the lattice parameter is reduced by 2%, which is in good agreement with the observed 10% increase in NiO. These results for VO also show that Δ is very nearly proportional to the total $3d$ bandwidth.

In addition to Δ , it is useful to consider the values for the Racah parameters B and C that are determined from the absorption spectra for MnO, CoO, and NiO. These parameters are important because they measure the Coulomb repulsion between electrons in the free ion or the crystal. A comparison between the crystalline and free-ion values³⁵ is contained in Table II. It is well known that the crystalline Racah parameters are reduced relative to their free-ion values. This reduction is attributed either to an expansion of the d orbitals in the crystalline environment³⁷ or to a renormalization effect that is due to the fact that overlap and covalency can reduce the normalization factor of a molecular orbital to a value less than 1.³⁸ From the results of Table II, we can determine empirical estimates of the F^2 and F^4 integrals in the solid and calculate Δ_{ex} from Eq. (7). If $(q_+, -q_-) = 5, 4, 3,$ and 2 for MnO, FeO, CoO, and NiO, respectively, then this calculation yields the result that $\Delta_{\text{ex}} = 0.32, 0.27, 0.22,$ and 0.15 Ry for these compounds. The values for MnO and NiO are about half those calculated by Wilson²⁸ in his spin-polarized band calculation. This is consistent with Slater's observation that the Hartree-Fock and Hartree-Fock-Slater approximations tend to overestimate the F^2 and F^4 integrals because they ne-

TABLE II. Comparison between Racah parameters B and C for MnO, CoO, and NiO and the free-ion values (cm^{-1}).

| | B | C | Reference |
|------------------|-------|--------|-----------|
| MnO | 600 | 3550 | 10, 11 |
| Mn ²⁺ | 860 | 3850 | 34 |
| FeO | (690) | (3650) | a |
| Fe ²⁺ | 917 | 4040 | 34 |
| CoO | 750 | 3760 | 9 |
| Co ²⁺ | 971 | 4500 | 34 |
| NiO | 800 | 4000 | b |
| Ni ²⁺ | 1030 | 4850 | 34 |

^aEstimated by interpolation.

^bEstimated from the data of Newman and Chrenko, Ref. 12.

glect correlation effects.²⁷

The present interpretation of the crystal-field parameter Δ indicates that the 3d bands in MnO, FeO, CoO, and NiO are about 3 to 4 eV wide. It was shown in I that this is about the width one would expect from a comparison with the 3d bandwidth in metallic nickel, where the nearest-neighbor nickel-nickel distance is about 20% smaller than it is in the oxide. This is undoubtedly a more realistic estimate of the 3d bandwidths in these materials than that of Adler and Feinleib,²⁵ who estimate 3d bandwidths that are a few hundredths of an electron volt. The magnitude of the 3d bandwidth is an important factor in Hubbard's approximate treatment of correlation effects in narrow-band materials.²⁶ In the case of a half-filled s band, Hubbard has shown that a Mott transition occurs when the bandwidth W is comparable with U , the Coulomb repulsion energy between two electrons on the same atom. Anderson³⁹ has estimated that $U = 9 \pm 2$ eV for the latter members of the 3d transition series. Adler and Feinleib²⁵ estimate that $U = 13$ eV in NiO. These results suggest that the ratio W/U is about 0.3 or 0.4, which according to Hubbard's simplified model calculation, predicts that these compounds are Mott insulators.

Powell and Spicer⁴⁰ have measured the reflectance spectra of NiO and CoO over an energy range extending from 1 to 26 eV. They observe an absorption edge near 3.7 eV in both materials, some small structure up to 9 eV, and then two larger peaks near 14 and 18 eV. They propose two possible explanations for the absorption edge at 3.7 eV. These models involve either 2p-3d or 3d-4s,4p transitions. Adler and Feinleib²⁵ favor the latter interpretation. Ksendzov and Drabkin⁴¹ have observed photoconductivity above 4 eV in NiO, but similar studies by Powell and Spicer⁴⁰ indicate that this may be a surface rather than a bulk effect. Photoemission studies by Powell and Spicer indicate that the structure at 14 and 18 eV in NiO is due to transitions from states 6 and 9 eV below the Fermi level to unoccupied states that are about 8 eV above the Fermi energy. Adler and Feinleib interpret the 14-eV peak in terms of $d^8 + d^8 - d^7 + d^9$ transitions and the 18-eV peak to 2p-3d excitations.

It is likely that the 3.7 eV absorption edge in these oxides involves transitions from localized 3d to itinerant 4s-4p states. According to the results of Tables III and VI of I, the energies of the e_g and t_{2g} Wannier functions are about 2 eV below the bottom of the 4s band in NiO. However, this separation gradually decreases as one moves from NiO to MnO until finally, the e_g and t_{2g} energies straddle the bottom of the 4s band in MnO. Although the actual magnitude of this gap could be underestimated in the present calculations, the relative changes from one compound to another

are probably quite reliable. This appears to contradict the fact that the absorption edges in MnO and NiO both occur at about 3.7 eV.

Slater and Wood⁴² have questioned the validity of interpreting optical excitation energies in terms of differences in one-electron energies when the statistical exchange or $X\alpha$ method is applied. They find that differences in the one-electron energies are related to differences in the total energy of the crystal only when the initial and final states are itinerant Bloch functions. They suggest that optical excitations in semiconductors and insulators involve localized holes, and these must be treated in a way analogous to the theory of optical excitations in isolated atoms. As an example, they consider the case of the chromium atom. They show that although the one-electron energy for a 4s electron is lower than that of a 3d electron, the difference in total energies between the $3d^4 4s^2$ and $3d^5 4s$ configurations is positive. Similar effects could account for the observed 3.7-eV absorption edge in MnO and NiO. These effects would also dominate the optical properties at higher energies, thereby complicating the relationship between the observed optical properties and the calculated one-electron band structure.

Despite these uncertainties regarding the validity of the one-electron model for interpreting the 3d-4s absorption edge in these compounds, it is interesting to estimate the extent to which correlation effects could lower the 3d one-electron energies. The first estimate involves the exchange splitting between the spin-up and spin-down bands in the spin-polarized method, which is given by Δ_{ex} in Eq. (7). Slater²⁷ has shown that Δ_{ex} is $\frac{6}{5}$ times the difference between the average energy of multiplets with total spins $S-1$ and S . Thus, we can use Δ_{ex} to estimate the effect of Hund's rule coupling on the one-electron energies. Since Δ_{ex} will split the nonmagnetic energy bands symmetrically, the one-electron energy is reduced by $\frac{1}{2}\Delta_{ex}$ in MnO since only the lower subband is occupied. In FeO, CoO, and NiO, additional electrons are added to the upper bands so that, on the average, the one-electron energies are reduced by the factors $\frac{1}{3}$, $\frac{3}{4}$, and $\frac{1}{8}$ times the corresponding values for Δ_{ex} . Using the previously estimated values for Δ_{ex} , this effect lowers the energy of the 3d Wannier functions by 0.16 Ry in MnO and 0.02 Ry in NiO. This tends to equalize the energy gaps in these materials but leaves it somewhat smaller than the experimental value of 3.7 eV.

A second method for estimating the effects of correlation on the 3d one-electron energies has been suggested by Brinkman.⁴³ This method is based on the Hubbard model for treating correlation effects in narrow-band materials.²⁷ According to this model, electron-electron interactions will

split the nonmagnetic $3d$ bands for a d^n configuration into n occupied bands which are separated by an energy U from $(10-n)$ unoccupied bands. In the nonmagnetic band structure, the Coulomb interaction is overestimated by the assumption that each of the ten $3d$ spin orbitals is equally occupied by $(n/10)$ electrons. As a result, the Coulomb interaction between a given electron with the other electrons in the remaining nine d orbitals leads to a Coulomb interaction energy of $(9n/10)U$. When correlation effects are taken into account via the Hubbard model, the Coulomb energy is $(n-1)U$ for the occupied states, since the electron does not interact with itself. However, the unoccupied states have a Coulomb energy of nU . Thus, these correlation effects will lower the band energies by the difference $(9n/10)U - (n-1)U$ or $(1-n/10)U$, where the factor $(1-n/10)$ equals 0.5, 0.4, 0.3, and 0.2 for MnO, FeO, CoO, and NiO, respectively. Thus, this model can readily explain a 3.7-eV absorption edge in both MnO and NiO with a value for U in the 6–8-eV energy range.

Finally, we consider the question of ionicity in these materials. Adler and Feinleib²⁵ and others claim that these transition-metal monoxides are very near the fully ionic limit since the covalency parameters for MnO and NiO have been shown by Fender *et al.*⁴⁴ to be less than 4%. Fender *et al.* estimate that these covalency effects reduce the charge on the metal atoms from the fully ionic value of +2 to about +1.8. Yet, Gielisse *et al.*⁴⁵ have determined the effective charge q^* in CoO and NiO from the reststrahlen spectra, and they obtain values for q^* in the +0.84 to +0.89 range. Thus, we have an apparent discrepancy of about one unit of electronic charge between these two independent measurements of the ionicity in these compounds.

We suggest a very simple explanation for this apparent discrepancy. The neutron-diffraction measurements of the magnetic scattering in MnO

and NiO by Fender *et al.* determine the extent to which covalent mixing occurs between the metal $3d$ and the oxygen $2s$ and $2p$ orbitals. It has been suggested in I that these covalency effects represent only a small fraction of those responsible for the total charge distribution in these compounds. A similar but much stronger mixing occurs between the metal $4s-4p$ and the oxygen $2s-2p$ orbitals, and this $s-p$ mixing could easily reduce the effective charge on the metal atoms from the +1.8 to the +0.8–0.9 range.

The present LCAO model has been applied to estimate the extent to which covalent mixing between the metal $3d$ and the oxygen $2s$ and $2p$ orbitals will reduce the ionicity in these monoxides. Using the LCAO parameters for NiO that are given in Table IV of I, the LCAO charge distribution has been calculated by sampling the occupied bands at 2048 points in the fcc Brillouin zone. This calculation predicts that the nickel atoms have a charge of +1.7, which is in satisfactory agreement with the neutron-diffraction estimate of +1.8. If the LCAO method were generalized to include the metal $4s-4p$ orbitals, the strong metal-ligand overlap and covalency effects that would be required to raise the metal $4s-4p$ bands an estimated 6 eV could easily reduce the total ionic charge on the metal atoms to the +0.8–0.9 range. This result indicates that our initial assumption that these compounds are neutral rather than ionic is not rigorously correct. However, it does suggest that the neutral-atom model is a more realistic starting point for a self-consistent band calculation than the fully ionic model.

ACKNOWLEDGMENTS

I want to acknowledge several useful and informative conversations with W. F. Brinkman and V. Heine on various aspects of this work.

¹L. F. Mattheiss, preceding paper, Phys. Rev. B **5**, 290 (1972).

²R. C. Whited and W. C. Walker, Phys. Rev. **188**, 1380 (1969).

³J. A. Van Vechten, Phys. Rev. **187**, 1007 (1969).

⁴J. Janin and L. Cotton, Compt. Rend. **246**, 1936 (1958).

⁵F. J. Morin, Phys. Rev. Letters **3**, 34 (1959).

⁶I. G. Austin, Phil. Mag. **7**, 961 (1962).

⁷M. D. Banus and T. B. Reed, in *Proceedings of the Symposium on the Chemistry of Extended Defects in Non-Metallic Solids* (North-Holland, Amsterdam, 1970).

⁸N. J. Doyle, J. K. Hulm, C. K. Jones, R. C. Miller and A. Taylor, Phys. Letters **26A**, 604 (1968).

⁹G. W. Pratt, Jr., and R. Coelho, Phys. Rev. **116**, 281 (1959).

¹⁰D. R. Huffman, R. L. Wild, and M. Shinmei, J. Chem. Phys. **50**, 4092 (1969).

¹¹R. N. Ishenderov, I. A. Drabkin, L. T. Emel'yanova, and Ya. M. Ksendzov, Fiz. Tverd. Tela **10**, 2573 (1969) [Sov. Phys. Solid State **10**, 2031 (1969)].

¹²R. Newman and R. M. Chrenko, Phys. Rev. **114**, 1507 (1959).

¹³D. R. Stephens and H. G. Drickamer, J. Chem. Phys. **34**, 937 (1961).

¹⁴D. Reinen, Ber. Bunsenges Phys. Chem. **69**, 82 (1965).

¹⁵W. Low, Phys. Rev. **109**, 247 (1958).

¹⁶W. Low, Phys. Rev. **109**, 256 (1958).

¹⁷J. Yamashita, J. Phys. Soc. Japan **18**, 1010 (1963).

¹⁸A. C. Switendick, Ph.D. thesis (MIT, Massachusetts, 1963) (unpublished); J. Appl. Phys. **37**, 1022 (1966).

¹⁹V. Ern and A. C. Switendick, Phys. Rev. **137**, A1927 (1965).

²⁰J. M. Schoen and S. P. Denker, Phys. Rev. **184**,

- 864 (1969).
- ²¹T. E. Norwood and J. L. Fry, *Phys. Rev. B* **2**, 472 (1970).
- ²²N. F. Mott, *Proc. Phys. Soc. (London)* **A62**, 416 (1949).
- ²³F. J. Morin, *J. Appl. Phys.* **32**, 2195 (1961).
- ²⁴D. Adler, in *Solid State Physics*, edited by F. Seitz, D. Turnbull, and H. Ehrenreich (Academic, New York, 1968).
- ²⁵D. Adler and J. Feinleib, *Phys. Rev. B* **2**, 3112 (1970).
- ²⁶J. Hubbard, *Proc. Roy. Soc. (London)* **A281**, 401 (1964).
- ²⁷J. C. Slater, *Phys. Rev.* **165**, 658 (1968); *J. Appl. Phys.* **39**, 761 (1968).
- ²⁸T. M. Wilson, *Intern. J. Quantum Chem.* **25**, 269 (1968); *J. Appl. Phys.* **40**, 1588 (1969); *Intern. J. Quant. Chem.* **3**, 757 (1970).
- ²⁹V. Heine and L. F. Mattheiss, *J. Phys. C* **4**, L191 (1971).
- ³⁰L. F. Mattheiss, *Phys. Rev. B* **2**, 3918 (1970).
- ³¹W. H. Kleiner, *J. Chem. Phys.* **20**, 1784 (1952).
- ³²C. Y. Fong, W. Saslow, and M. L. Cohen, *Phys. Rev.* **168**, 922 (1968).
- ³³D. W. Fischer, *J. Appl. Phys.* **41**, 3922 (1970).
- ³⁴C. Herring, in *Magnetism*, edited by G. T. Rado and H. Suhl (Academic, New York, 1966).
- ³⁵S. Sugano, Y. Tanabe, and H. Kamimura, *Multiplets of Transition-Metal Ions in Crystals* (Academic, New York, 1970).
- ³⁶R. L. Clendenen and H. G. Drickamer, *J. Chem. Phys.* **44**, 4223 (1966).
- ³⁷W. Marshall and R. Stuart, *Phys. Rev.* **123**, 2048 (1961).
- ³⁸S. Koide and M. H. L. Pryce, *Phil. Mag.* **3**, 607 (1958).
- ³⁹P. W. Anderson, in *Solid State Physics*, edited by F. Seitz and D. Turnbull (Academic, New York, 1963).
- ⁴⁰R. J. Powell and W. E. Spicer, *Phys. Rev. B* **2**, 2182 (1970).
- ⁴¹Ya. M. Ksendzov and I. A. Drabkin, *Fiz. Tverd. Tela* **7**, 1519 (1965) [*Sov. Phys. Solid State* **7**, 1220 (1965)].
- ⁴²J. C. Slater and J. H. Wood, *Intern. J. Quantum Chem.* **4**, 3 (1971).
- ⁴³W. F. Brinkman (private communication).
- ⁴⁴B. E. F. Fender, A. J. Jacobson, and F. A. Wedgwood, *J. Chem. Phys.* **48**, 990 (1968).
- ⁴⁵P. J. Gielisse, J. N. Plendl, L. C. Mansur, R. Marshall, S. S. Mitra, E. Mykolajewycz, and A. Smakula, *J. Appl. Phys.* **36**, 2446 (1965).

Electronic Band Structure of Niobium Nitride

L. F. Mattheiss

Bell Laboratories, Murray Hill, New Jersey 07974

(Received 5 August 1971)

The augmented-plane-wave method is applied to calculate the electronic band structure of niobium nitride (NbN). The results are qualitatively similar to those obtained from previous energy-band calculations for the 3d transition-metal monoxides which form with the same rocksalt structure. The Fermi level for NbN falls in the lower portion of the t_{2g} manifold of the niobium 4d bands so that the conduction electrons in NbN are predominantly 4d-like in character. These results are compared with some of the previous band-structure models that have been proposed to explain the electronic properties of NbN and other closely related refractory hard metals with the rocksalt structure.

I. INTRODUCTION

Niobium nitride is one of a family of refractory "hard metals" that can be formed by combining boron, carbon, or nitrogen with Group-IV, -V, and -VI transition-series elements. These compounds are characterized by high melting points, hardness, brittleness, and resistivities comparable to those observed in good metals.¹ In addition, these compounds include materials with high superconducting transition temperatures, and these transition temperatures are found to vary significantly with composition.

Geballe *et al.*² have measured the superconducting transition temperatures, lattice parameters, low-temperature heat capacities, and magnetic susceptibilities of the niobium nitride-carbide system. They have found unusually small values for the

electronic heat-capacity coefficient and the magnetic susceptibility in these compounds. This has led them to propose an energy-band model for NbN containing niobium 5s-5p and nitrogen 3s-3p electrons at the Fermi level, with the niobium 4d bands above the Fermi energy and therefore unoccupied.

A variety of band-structure models had been proposed previously to explain the physical properties of these materials. One of the original ideas was suggested by Hägg³ about 40 years ago. Hägg proposed that these materials could be regarded as interstitial alloys rather than compounds, with the nonmetal atoms merely filling the voids in the host lattice of transition-metal atoms. As a result of this model, these materials are frequently referred to as "interstitial" compounds. This simple idea has been refined and improved over the years, and two distinct models have emerged.¹ The first